Signatures of nematic superconductivity in doped Bi₂Se₃ under applied stress

Pye Ton How

Institute of Physics, Academia Sinica, Taipei 115, Taiwan

Sung-Kit Yip

Institute of Physics, Academia Sinica, Taipei 115, Taiwan;
Institute of Atomic and Molecular Sciences, Academia Sinica, Taipei 106, Taiwan;
and Physics Division, National Center for Theoretical Sciences, Hsinchu 300, Taiwan

The $M_x\text{Bi}_2\text{Se}_3$ family are candidates for topological superconductors, where M could be Cu, Sr, or Nb. Twofold anisotropy has been observed in various experiments, prompting the interpretation that the superconducting state is nematic. However, it has since been recognized in the literature that a twofold anisotropy in the upper critical field H_{c2} is incompatible with the naive nematic hypothesis. In this paper we study the Ginzburg-Landau theory of a nematic order parameter coupled with an applied stress, and classify possible phase diagrams. Assuming that the H_{c2} puzzle is explained by a preexisting "pinning field," we indicate how a stress can be applied to probe an extended region of the phase diagram, and verify if the superconducting order parameter is indeed nematic. We also explore the Josephson tunneling between the proposed nematic superconducting state and an *s*-wave superconductor. The externally applied stress is predicted to serve as an on/off switch to the tunneling current, and in a certain regime the temperature dependence of the critical current can be markedly different from that between two conventional *s*-wave superconductors.

I. INTRODUCTION

Bi₂Se₃ is a topological insulator [1–3]. When intercalated with electron-donating atoms such as Cu [4,5], Sr [6], or Nb [7,8], it becomes superconducting at low temperature. Following their identification as candidates of topological superconductors [9–11], the family of materials has recently garnered a lot of interest [12]. Experimentally, twofold anisotropy in the superconducting phase has been observed in NMR Knight's shift [13], specific heat [14–16], magnetic torque [8], magnetotransport, and upper critical field [14,17–19]. This is incompatible with the crystal lattice symmetry, and has led to the hypothesis that the superconducting state is nematic in nature, i.e., it spontaneously breaks both lattice rotational and gauge symmetries. While the superconductivity is suppressed by an applied hydrostatic pressure [20,21], the twofold anisotropy is observed as far as superconductivity holds [21].

The parent material Bi₂Se₃ forms a rhombohedral crystal, with a lattice point group D_{3d}; see Fig. 1. According to the nematic hypothesis, the complex superconducting order parameter $\vec{\eta}$ is believed to transform under the irreducible representation E_u [10], which is parity odd and two dimensional, and, in the absence of other symmetry breaking effect, spontaneously breaks the crystal rotation symmetry together with the $U(1)$ symmetry. It can be thought of as a nematic director in the basal plane, since $\vec{\eta}$ and $-\vec{\eta}$ can be identified up to a global $U(1)$ phase shift of π. Experiments that detect the anisotropy in the basal plane all reported a twofold symmetry, consistent with the presence of a nematic superconducting order parameter. This naive picture, however, is contradicted by several pieces of experimental facts.

First of all, the upper critical field H_{c2} is experimentally observed to be *twofold* anisotropic [14,16–19] with the applied field parallel to the basal plane, seemingly inline with other measurements. However, this result is actually incompatible with the naive nematic hypothesis, which indicates a *sixfold* anisotropy for H_{c2} [22–24].

To understand this, one considers the *onset* of superconductivity in high field. Instead of a finite $\vec{\eta}$ providing a preferred orientation, the magnetic field and the lattice anisotropy together determine the orientation of the infinitesimal $\vec{\eta}$ when it first emerges. This consideration leads to the prediction of a sixfold anisotropy associated with the sixfold improper rotation symmetry of D_{3d}.

The robustness of the twofold nematic direction observed in experiments is another puzzle unexplained by the naive nematic scenario. It was noted that the twofold anisotropy for a given sample is always pinned at the same direction. In Pan *et al.* [17] part of the experiment was performed with the sample repeatedly cycled up to 5 K (about $1.6T_c$) and cooled back down to superconducting phase again before every field sweep [25]. In a separate account [26], the same twofold direction for any given sample persists as it was cycled in and out of the superconducting phase repeatedly, sometimes all the way to room temperature and back, with or without a background magnetic field. To account for this behavior, the rotational symmetry must have been already broken in some way at room temperature.

Indeed, for the case of Sr, evidence of normal-state nematic response was reported by Kuntsevich *et al.* [27] and Sun *et al.* [16]. On the other hand, the Argonne group [15,19] reported an isotropic normal-state response for Sr. This is in contrast
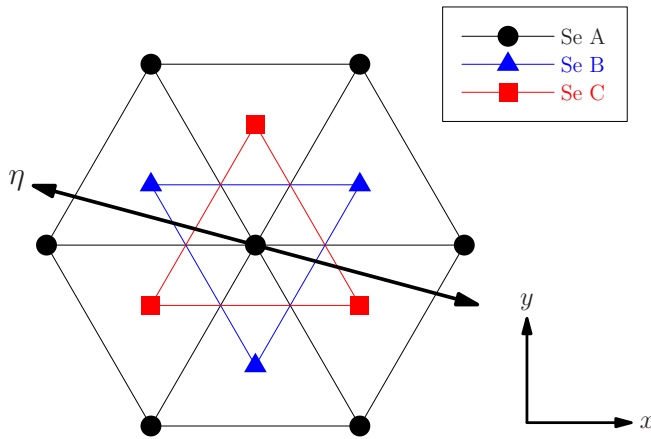
FIG. 1. The positions of the selenium atoms within a quintuple layer of Bi_2Se_3. The superconducting order parameter $\vec{\eta}$ is shown here pointing in an arbitrary direction.

with the case of Cu, where no nematicity was ever observed above T_c [13,14] to our knowledge.

To reconcile the E_u pairing scenario and the observed robust pinning effect, some nematic symmetry-breaking field (SBF) must already be present in the sample [15]. The precise nature of this SBF is yet unknown, though mechanical stress or strain were named as possible candidates [10]. This SBF pins all the twofold nematic responses (including H_{c2}) in the same direction for a given sample.

We emphasize that any scenario that solely relies on spontaneous symmetry breaking at low temperature to supply the nematic direction is incompatible with experiments. The naive nematic scenario does not work, nor does any scenario where the rotational symmetry is broken independent of the $U(1)$ symmetry, for example [28]. A preexisting SBF ("pinning field") is necessary.

A conceptual difficulty then arises: in the presence of a pinning field, an otherwise isotropic s-wave superconductor can in principle also appear twofold anisotropic. Can we tell this so-called anisotropic s-wave scenario apart from the true nematic scenario? This distinction is more than merely academic, because the nematic superconductor is topological [10,11], while the s-wave case is not.

In light of these recent developments, a better understanding of how the proposed nematic superconductivity interacts with an explicit SBF is clearly desirable. In this work we consider mechanical stress or strain as the prototypical SBF, although an SBF with a different microscopic nature will have exactly the same phenomenology. We further consider the application of stress in addition to the existing, unknown SBF, as an experimental probe of the nature of the superconducting phase.

Historically, much of the phenomenology of a superconducting order parameter with nontrivial symmetry has been known as part of the lore of the unconventional superconductors (see Refs. [29,30] and references therein.) Pertinent to the present discussion is the fact that, due to the competition of the SBF and the crystal field, the superconducting transition may be split into two if the order parameter is multicomponent [31,32]. In the heavy fermion compound UPt_3, the double

transition is due to the antiferromagnetic order in the normal state, and has been experimentally observed [33]. The idea of a stress causing a similar split has been put forward for Sr_2RuO_4 [34,35], but to our knowledge has never been observed [36,37].

In this paper we formulate the Ginzburg-Landau (GL) theory of a nematic superconducting order parameter coupled to an external SBF, and explore the phenomenology as a guide to future experiments. In particularly, following the suggestion of [10], we consider stress as the prototypical SBF. The GL theory is written down in Sec. II, and then in Secs. III, IV, and V we identify the splitting of the superconducting transition, as well as another possible transition at a lower temperature, and classify possible phase diagrams as function of stress and temperature. In Sec. VI we further explore the phenomenology when the system is subjected to two SBFS: a preexisting pinning field and a stress applied as an experimental probe, and propose experimental signatures that may help distinguish a truly nematic superconducting order parameter from a single-component one.

In addition, in Sec. VII we consider the critical tunnel current in the Josephson junction between the proposed nematic superconducting state and another s-wave superconductor. The idea of using the Josephson effect as a probe for unconventional pairing symmetry has long been considered [38–42]. The Ginzburg-Landau approach is also applicable to describe the Josephson tunneling [43]. If the nematic hypothesis does hold, the critical current shows a nontrivial anisotropic dependence on the SBF, as well as a temperature dependence that differs from the s-wave-to-s-wave scenario. This provides another experimental test for the nematicity.

II. GINZBURG-LANDAU FREE ENERGY

We will formulate the GL theory by treating the system as "almost D_{3d} invariant." That is, we consider the nematic superconducting order parameter living in the E_u representation of D_{3d}, and write down a D_{3d}-invariant free energy. The pinning effect is introduced via coupling to a (possibly weak) explicit SBF.

This scenario is similar to the nematic pseudogap phase of YBCO [44–47], where the order parameter would have broken the fourfold rotation symmetry of the CuO_2 plane, except that this "symmetry" is already weakly broken by the orthorhombic lattice. Nonetheless, the nematic response is greatly enhanced by the nematic pseudogap order parameter.

A. Free energy without SBF

Let us first give a brief recap of the GL free energy for a nematic superconductor in the absence of any SBF.

We define the coordinate axes as follows: the z axis is aligned with the principal C_3 axis of the lattice, the x axis is along one of the C_2 axes in the basal plane, and the y axis is chosen to form a right-handed set of a coordinate system.

We assume that the superconducting order parameter is a complex two-component quantity $\vec{\eta}$. It will be parametrized as

$$\vec{\eta} = \begin{pmatrix} \eta_x \\ \eta_y \end{pmatrix} = \sqrt{D} \begin{pmatrix} \cos\theta \\ e^{i\phi}\sin\theta \end{pmatrix}. \tag{1}$$

Here η_x is kept real by a suitable global $U(1)$ phase rotation. See Fig. 1 for illustration.

The point group D_{3d} can be built from three operations: $2\pi/3$ rotation about the z axis (denoted C_3), π rotation about the x axis (denoted C_2'), and mirror reflection about the yz plane (denoted M). The odd-parity proposal [10] would have $\vec{\eta}$ transforming in the E_u representation, similar to (x, y).

However, we may equally well consider the possibility where $\vec{\eta}$ transforms in the E_g representation instead, similar to the pair $(yz, -xz)$. Gauge invariance requires $\vec{\eta}$ and $\vec{\eta}^*$ to always come in pairs in the GL expansion, and the sign of parity is irrelevant. The GL free energy and most of the subsequent analysis remain unchanged for the E_g scenario, except that a minor modification is needed for the Josephson tunneling, which does not affect our qualitative conclusion. For either case, one can consistently define η_x to be the component invariant under C_2'.

The quantity $\vec{\eta}$ is to be considered as a headless vector, since a sign in $\pm\vec{\eta}$ can be regarded as a $U(1)$ phase factor. Therefore one may restrict θ to the interval $(-\pi/2, \pi/2]$, keeping in mind that θ and $\theta + \pi$ are always degenerate.

The GL expansion of free energy is obtained by writing down all the terms that are invariant under D_{3d}, global phase shift of $\vec{\eta}$, and time reversal. Up to $O(\eta^6)$, the most generic form is

$$\mathcal{F}_0 = \alpha|\eta|^2 + [\beta_1'|\eta|^4 + \beta_2'(\vec{\eta}\cdot\vec{\eta})(\vec{\eta}^*\cdot\vec{\eta}^*)]$$
$$+ \{\gamma_1'|\eta|^6 + \gamma_2'[(\eta_1 + i\eta_y)^3(\eta_x^* + i\eta_y^*)^3$$
$$+ (\eta_x - i\eta_y)^3(\eta_x^* - i\eta_y^*)^3] + \gamma_3'|\eta|^2(\vec{\eta}\cdot\vec{\eta})(\vec{\eta}^*\cdot\vec{\eta}^*)\}.$$
(2)

Here α is taken to be

$$\alpha = \kappa\left(\frac{T - T_0}{T_0}\right),$$
(3)

where T_0 is the superconducting transition temperature without external field. We ignore the temperature dependence of all other coefficients.

Let us first consider the free energy up to $O(\eta^4)$. To this order $\mathcal{F}_0$ is in fact invariant under arbitrary rotations in the xy plane. Two solutions for $\vec{\eta}$ are possible: the complex chiral state that is rotationally invariant but spontaneously breaks time-reversal symmetry, and the real nematic state which breaks the rotational symmetry but is time-reversal invariant. The sign of β_2' decides which phase is favored [48,49].

Since the nematic state is by assumption the true solution, we take the appropriate sign $\beta_2' < 0$. The minimum of $\mathcal{F}$ now lies along $\phi = 0$, and in effect $(\vec{\eta}\cdot\vec{\eta})(\vec{\eta}^*\cdot\vec{\eta}^*) = |\eta|^4$. Therefore we define $\beta \equiv \beta_1' + \beta_2'$, and require $\beta > 0$ for stability.

Now let us move on to include terms of $O(\eta^6)$. The γ_3' term essentially has the same θ and ϕ dependence as the β_2' term. Since a transition from nematic to chiral state at a lower temperature is never observed, we explicitly require $\gamma_3' < 0$. On the other hand, it can be shown that all extrema of the γ_2' term correspond to real values of $\vec{\eta}$. Consequently, one may assume $\vec{\eta}$ is real and simply set $\phi = 0$. In terms of θ and D, the free energy reads

$$\mathcal{F}_0 = \alpha D + \beta D^2 + [\gamma_1 + \gamma_2\cos(6\theta)]D^3,$$
(4)

where $\gamma_1 \equiv \gamma_1' + \gamma_3'$ and $\gamma_2 = 2\gamma_2'$. For stability we require $\gamma_1 > 0$ and $\gamma_1 > |\gamma_2|$.

The γ_2 term breaks the full rotational symmetry down to a discrete sixfold symmetry. This is the lowest order at which the crystal anisotropy enters the GL expansion [49].

B. Stress as an SBF

Stress serves as our prototypical SBF. We will focus on stress in the xy plane. Generally, planar stress is a rank-two symmetric tensor $\hat{\varepsilon}$ with three independent real parameters. Under D_{3d}, this tensor decomposes into two parts: the scalar $\mathrm{Tr}\,\hat{\varepsilon}$, and the traceless part which is organized to form the two-component quantity

$$\vec{\varepsilon} = \begin{pmatrix} \varepsilon_{xx} - \varepsilon_{yy} \\ -2\varepsilon_{xy} \end{pmatrix} \equiv \begin{pmatrix} \varepsilon_1 \\ \varepsilon_2 \end{pmatrix} = \varepsilon\begin{pmatrix} \cos[2(-\Phi + \Phi_0)] \\ \sin[2(-\Phi + \Phi_0)] \end{pmatrix}, \quad (5)$$

which transforms in the E_g representation under D_{3d}.

Gauge invariance of the free energy requires that $\vec{\eta}$ and $\vec{\eta}^*$ pair up, and all allowed combinations are parity even. Therefore to couple to the nematic superconductor at all, an SBF must transform under the even-parity E_g representation. It therefore shares the same phenomenology with stress (5). One can simply replace the stress with any preexisting SBF of an arbitrary origin, and the resulting GL free energy is formally identical. In particular, we note that for externally applied *strain*, the form of GL free energy (14) remains exactly identical. The result in this paper equally applies to experiments which uses strain instead of stress.

We choose to parametrize $\vec{\varepsilon}$ as (5) because Φ would correspond to the physical rotation angle about the z axis. When the stress is rotated by an arbitrary angle δ, $\vec{\varepsilon}$ changes via $\Phi \to \Phi + \delta$. The angle Φ_0 defines the direction relative to the x axis that corresponds to $\Phi = 0$, and we leave it unspecified for now, to be chosen for convenience later. The angle Φ defines a special direction in the basal plane, and subsequently we may refer to it as the "orientation" of the stress. This breaks the point group rotation symmetry.

For the sake of completeness, we state that one can form another E_g pair using out-of-plane stress components: the pair $(\varepsilon_{yz}, -\varepsilon_{xz})$ can be used in place of (5). Note that this is possible only for the trigonal D_3d group. If B and C sites in Fig. 1 were to be identified, the resultant hexagonal D_{6h} point group would not have allowed the replacement.

For the remainder of this paper, we will always assume that $\mathrm{Tr}\,\hat{\varepsilon}$ is kept constant. The dependence of GL coefficients on $\mathrm{Tr}\,\hat{\varepsilon}$ can therefore be entirely disregarded.

We will only consider coupling to $\vec{\varepsilon}$ at linear order. As discussed above, gauge invariance requires $\vec{\eta}$ and $\vec{\eta}*$ to comes in pairs that transform under the E_g representation. Up to order $O(\eta^4)$, the following is the exhaustive list of possible combinations:

$$\vec{S} = \begin{pmatrix} |\eta_x|^2 - |\eta_y|^2 \\ -\eta_x\eta_y^* - \eta_y\eta_x^* \end{pmatrix} \equiv \begin{pmatrix} S_1 \\ S_2 \end{pmatrix}, \quad (6)$$

$$\vec{T} = |\eta|^2\,\vec{S}, \quad (7)$$

$$\vec{U} = \begin{pmatrix} (|\eta_x|^2 - |\eta_y|^2)^2 - (\eta_x\eta_y^* + \eta_y\eta_x^*)^2 \\ 2(\eta_x\eta_y^* + \eta_y\eta_x^*)(|\eta_x|^2 - |\eta_y|^2) \end{pmatrix}. \quad (8)$$

The additional terms entering the free energy are

$$\mathcal{F}_\varepsilon = -g_0' \, \vec{\varepsilon} \cdot \vec{S} - g_1' \, \vec{\varepsilon} \cdot \vec{T} + g_2' \, \vec{\varepsilon} \cdot \vec{U}. \tag{9}$$

The leading $\vec{\varepsilon} \cdot \vec{S}$ term was considered in the literature [15,24]. We go beyond quadratic order in $\vec{\eta}$ to study the interplay between the applied stress and crystal anisotropy.

All three terms in (9) can be shown to be extremized by real values of $\vec{\eta}$. Together with (2), every term in the free energy favors a real $\vec{\eta}$. One is again allowed to set $\phi = 0$ from this point on.

Let us first look at $\vec{\varepsilon} \cdot \vec{S}$. Define $g_0 = |g_0'| > 0$. By appropriately choosing $\Phi_0 = 0$ or $\pi/2$, this term can be written as

$$-g_0' \, \vec{\varepsilon} \cdot \vec{S} = -g_0 \, \varepsilon D \cos(2\theta - 2\Phi). \tag{10}$$

The free parameter Φ_0 has been used up to fix the sign of g_0; now the $\vec{T}$ term must be taken as is. Define $g_1 = \pm g_1'$ with an appropriate sign depending on the previous choice of Φ_0, and one may write

$$-g_1' \, \vec{\varepsilon} \cdot \vec{T} = -g_1 \, \varepsilon D^2 \cos(2\theta - 2\Phi). \tag{11}$$

Similarly, the $\vec{U}$ term becomes

$$g_2' \, \vec{\varepsilon} \cdot \vec{U} = -g_2 \, \varepsilon D^2 \cos(4\theta + 2\Phi), \tag{12}$$

with $g_2 = \pm g_2'$ appropriately defined to absorb the possible sign due to the choice of Φ_0.

To sum up, the stress dependent part of GL free energy is

$$\begin{aligned} \mathcal{F}_\varepsilon &= -g_0 \cos(2\theta - 2\Phi)\varepsilon D \\ &\quad - [g_1 \cos(2\theta - 2\Phi) + g_2 \cos(4\theta + 2\Phi)]\varepsilon D^2. \end{aligned} \tag{13}$$

The coefficient g_0 is made positive by an appropriate choice of Φ_0. The other two coefficients g_1 and g_2 can be of either sign.

It can be seen that (4), (10), (11), and (12) are all invariant under sixfold (improper) rotation about the z axis. Consequently, we are free to impose the restriction $\Phi \in (-\pi/6, \pi/6]$, which amounts to redefining the x direction relative to the external stress.

The full expression of GL free energy $\mathcal{F}$ employed in this paper is the sum of (4) and (13). Let us also introduce another notation:

$$\mathcal{F} = \mathcal{F}_0 + \mathcal{F}_\varepsilon = aD + bD^2 + cD^3, \tag{14}$$

where a, b, and c are functions of α, θ, Φ, and ε.

C. Limit on the magnitude of stress

The explicit form of coefficient b in $\mathcal{F}$ is

$$b = \beta - g_1 \, \varepsilon \cos(2\theta - 2\Phi) - g_2 \, \varepsilon \cos(4\theta + 2\Phi). \tag{15}$$

If we take this expression at its face value, for ε large enough, the minimum value of b turns negative, and the transition from normal to superconducting state becomes first order.

While not implausible, this stress-induced first order transition has not been observed in any material to our knowledge. We therefore limit the range of ε in our theoretical investigation to avoid this regime. The appropriate condition is

$$\varepsilon \ll \frac{\beta}{|g_1|}, \frac{\beta}{|g_2|}. \tag{16}$$

D. Sign of γ_2

In the absence of an SBF, up to order D^2 the free energy $\mathcal{F}_0$ is symmetric under arbitrary rotation around the z axis. That is, η_x and η_y are completely degenerate. The sixfold symmetric γ_2 term breaks the degeneracy between η_x and η_y. When $\gamma_2 < 0$, the ground state has nonzero η_x, while $\gamma_2 > 0$ results in nonzero η_y [49].

Using a two-band lattice model, Fu [10] argued that η_y is the correct superconducting order parameter for $Cu_xBi_2Se_3$, which corresponds to $\gamma_2 > 0$. We will thus assume the positive sign for the remainder of the paper. However, we point out that all the result obtained subsequently can be easily mapped to the case where $\gamma_2 < 0$, should it turn out that way in experiment.

Let $\Delta\theta = \theta - \Phi$, and eliminate all occurrences of θ in favor of $\Delta\theta$ in (4) and (13). By shifting $\Phi \rightarrow \Phi + \pi/6$, one effectively reverses the signs of both γ_2 and g_2.

III. PHASE DIAGRAMS

In this section we will describe the three possible phase diagrams, assuming the GL free energy (14). The reduced temperature α, the magnitude of the stress ε, and the orientation of the stress Φ will span the three axes of the phase diagrams. The derivation and analysis of the features on these phase diagrams will be given in later sections.

We want to emphasize that any of the nontrivial structure of the phase diagram is a direct consequence of the nematic superconducting order parameter $\vec{\eta}$. An s-wave superconductor coupled to an explicit SBF may show anisotropic response, but will only exhibit a single superconducting phase, with T_c depending on $\vec{\varepsilon}$ analytically.

First let us consider the stress-free case $\varepsilon = 0$. The superconducting transition takes place at $\alpha = 0$, and the order parameter is sixfold rotationally degenerate: $\theta = -\pi/6, \pi/6$, or $\pi/2$. We will refers to these directions as the "natural minima" of the free energy.

Let us turn on the stress. By assumption, the size of stress ε is such that b remain positive for all values of θ and Φ. The normal-to-superconducting transition is then solely controlled by the coefficient a in (14):

$$a = \alpha - g_0 \, \varepsilon \cos(2\theta - 2\Phi). \tag{17}$$

At finite stress, the transition occurs at

$$\alpha = \alpha_1(\varepsilon) \equiv g_0 \, \varepsilon, \tag{18}$$

and the order parameter is directed at $\theta = \Phi$. We will refer to this as the *upper transition*.

A. $\Phi = 0$

We first examine the case when the direction of stress is fixed at $\Phi = 0$. This is a plane in the full three-dimensional parameter space $(\Phi, \varepsilon, \alpha)$.

We first orient the stress along $\Phi = 0$. Below T_c, the order parameter is locked to $\theta = 0$ by symmetry. This is labeled as phase A. As discussed earlier, the γ_2 term favors θ along one of the natural minima. The competition between g_0 and γ_2 eventually leads to a second order phase transition from $\theta = 0$ to $\theta \neq 0$ at a lower temperature $\alpha_2(\varepsilon)$. This will be referred to as
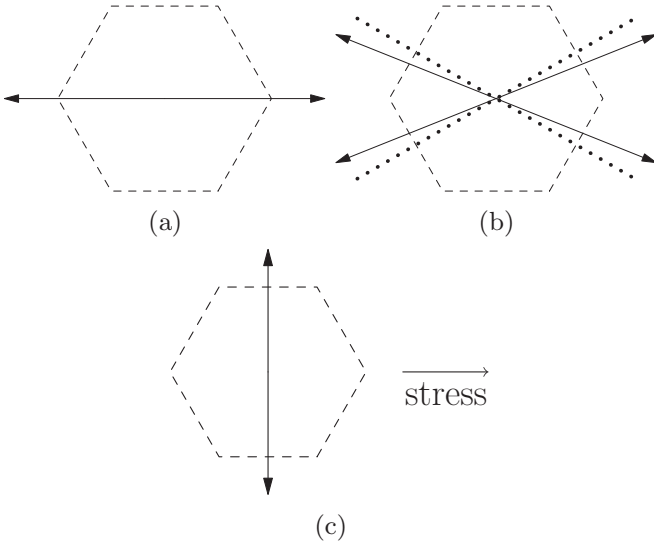
FIG. 2. The three allowed phases when the stress is oriented at $\Phi = 0$ as shown. (a) Phase A: immediately below the upper transition. (b) Phase B: between the middle and the lower transition if applicable. The two orientations depicted in phase B are degenerate and coexisting, and the dotted lines mark $\theta = \pm\pi/6$. (c) Phase C: below the possible lower transition.

as the *middle transition*. The lower temperature phase will be called phase B. See Fig. 2.

This can be explained in more physical terms. A hexagon has two types of high-symmetry directions. When the stress favors the x-type direction, but the naturally preferred orientation is of the y type (or vice versa), the middle transition exists as a result of the competition.

This middle transition only exists for $\Phi = 0$. Otherwise, θ will simply be pulled toward the nearer of $\pm\pi/6$ due to the reduced symmetry of the setup. At $\varepsilon = 0$, the upper and middle transition merge into a single superconducting transition.

Below $\alpha_2(\varepsilon)$, the $\Phi = 0$ plane is a first order coexistent surface, separating the $\theta > 0$ and $\theta < 0$ phases on either side. The middle transition is the critical end line of this surface.

Going still lower in temperature, another first order phase transition may occur at some $\alpha_3(\varepsilon)$, and forms the lower bound of the coexistence surface. It will be referred to as the *lower transition*. Below this lower transition, the orientation θ is fixed at $\pi/2$ (see Fig. 2). The necessary and sufficient condition for the lower transition is

$$g_1 < g_2. \tag{19}$$

The lower transition occurs at an temperature where $\vec{\eta}$ is no longer small. The sixth order γ_2 term dominates the free energy, and by the same argument g_0 is overwhelmed by g_1 and can be ignored. The γ_2 term has six degenerate minima [see Eq. (4)], and this degeneracy is lifted by g_1 and g_2. It will be shown subsequently that the difference $(g_1 - g_2)$ determines which of the six minima is most favorable, leading to the criterion (19).

All three lines of phase transition may continue indefinitely into higher stress, or alternatively the middle transition line may bend down and end when it merge with the lower
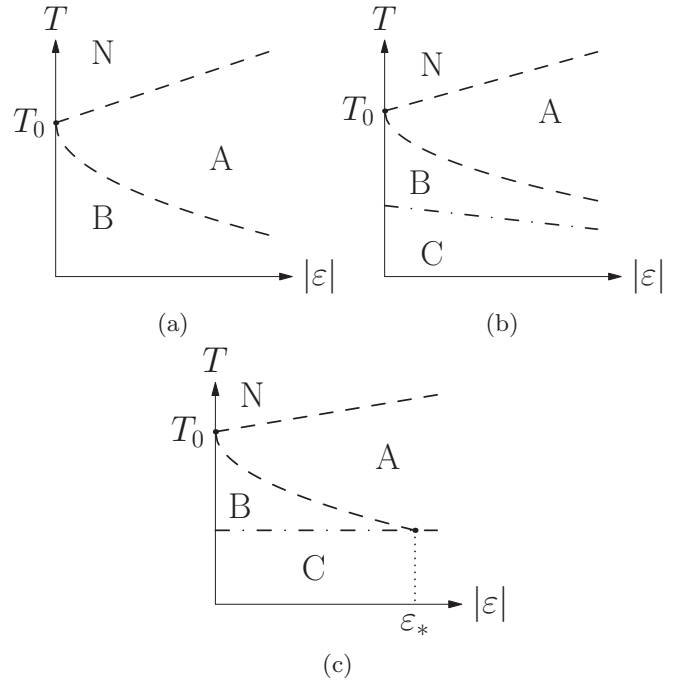

FIG. 3. The three possible phase diagrams when $\Phi = 0$. The dashed lines denote second order transitions, and the dash-dotted lines denote first order transitions. N denotes the normal phase. Note that the critical temperature T_2 of the middle transition is asymptotically $(T_2 - T_0) \propto \sqrt{\varepsilon}$ for small ε, as required by thermodynamics. (a) The lower transition is absent. (b) The lower transition is present. (c) The lower transition is present, and the middle transition merges with it at $\varepsilon = \varepsilon_*$.

transition at some value of stress ε_*. Overall, there are three different possible scenarios associated with this given $\mathcal{F}$ at $\Phi = 0$, as shown in Fig. 3.

B. $\Phi = \pi/6$

Immediately below the upper transition the order parameter has $\theta = \pi/6$, which is again locked by the symmetry. We shall refer to this as phase D. This orientation also minimizes the γ_2 term, however, and there is no middle transition.

On the other hand, the competition between g_0 and g_2 may be relevant at low temperature if (19) is satisfied, and then there is a lower transition. Crossing this transition from high to low temperature, the equilibrium state goes from $\theta = \pi/6$ to twofold degenerate $(\theta - \pi/6) > 0$ and $(\theta - \pi/6) < 0$. Please see Fig. 4 for illustration.

Purely from the symmetry standpoint, this transition can be of either first or second order. It will be shown that, for stress ε smaller than some critical value ε_c, the lower transition is of first order; beyond this point it becomes second order. We will let $\alpha_4(\varepsilon)$ denote the line of this lower transition.

Similar to the middle transition at $\Phi = 0$, lower transition here serves as the critical end line of a first order coexistent plane between the $\theta > \pi/6$ and $\theta < \pi/6$ phases on two sides of $\Phi = \pi/6$.

There are two possible scenarios at $\Phi = \pi/6$, one with and the other without a lower transition. The phase diagrams are as shown in Fig. 5.
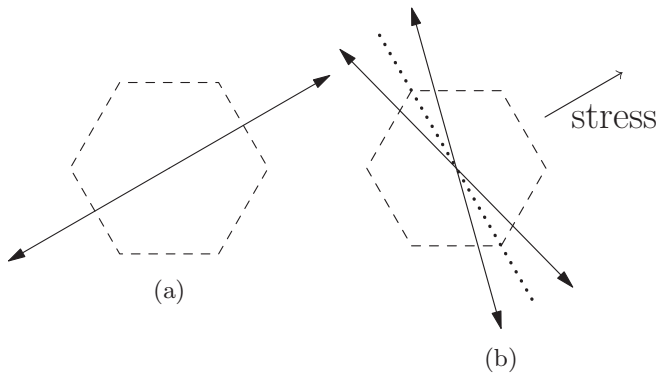
FIG. 4. The two allowed phases when the stress is oriented at $\Phi = \pi/6$. (a) Phase D: immediately below the upper transition. (b) Phase E: the phase below the lower transition if it is present. The dotted line marks the direction perpendicular to the stress.

C. The full phase diagram

A generic value of Φ breaks the sixfold rotational symmetry, and there cannot be a middle transition. If the (19) is satisfied, the resulting lower transition indeed span a first order coexistent surface, interpolating between the lines of lower transition we have identified at $\Phi = 0$ and $\Phi = \pi/6$. Overall there are three possible scenarios, as shown in Fig. 6.

As discussed earlier, the magnitude of stress in our discussion is limited by (16). Beyond the small-stress regime, the possible phase diagrams display very rich and complicated behaviors. But as noted above, this regime is unlikely to be physically relevant.

The middle transition at $\Phi = 0$ marks the temperature below in which γ_2 dominates over g_0. The lower transition is due to the competition between g_2 and γ_2. This already exhausts the list of possible competitions. Consequently we do not anticipate any other transition on the phase diagrams.

We have numerically verified the assertions made in this section. In the following sections we will present analytical derivations the phase diagrams, and analyze their experimental implications.
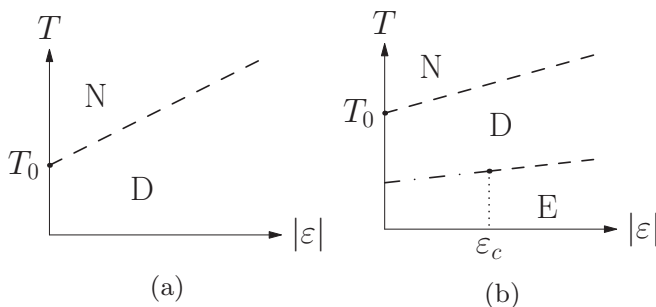

FIG. 5. The two possible phase diagrams when $\Phi = \pi/6$. The dashed lines represent second order transitions, and the dash-dotted line represents first order transition. N denotes the normal phase. (a) The phase diagram in the absence of a lower transition; and (b) the phase diagram in the presence of a lower transition. The lower transition change from first to second order at $\varepsilon = \varepsilon_c$.
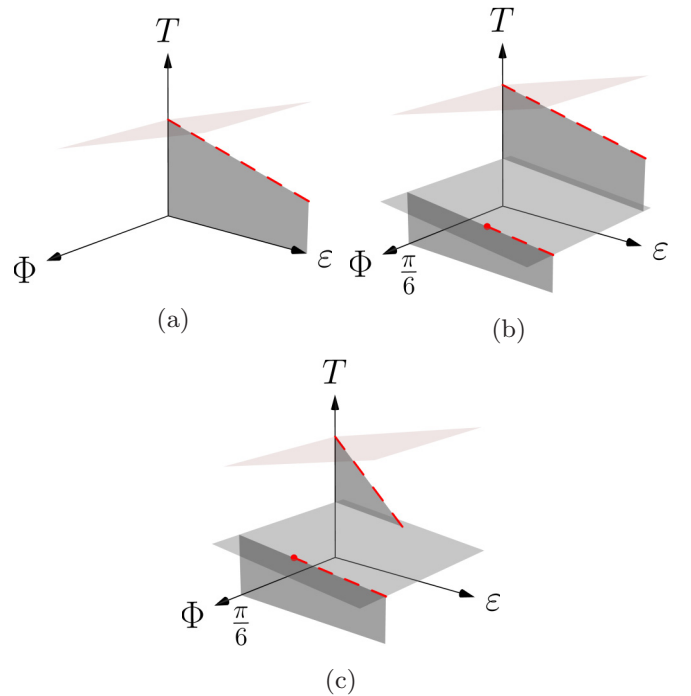

FIG. 6. The possible phase diagrams, with the Φ axis added. The upper shaded surface is the second order upper transition that separate normal and superconducting phases. The other shaded surfaces are first order coexistence surfaces, while the thick dashed line represents second order critical end lines. (a) Lower transition is absent. (b) Lower transition is present. (c) Lower transition is present, and the middle transition line ends on it.

IV. THE SPLIT SUPERCONDUCTING TRANSITION

A. Upper transition

The normal-to-superconducting transition occurs at $\alpha_1(\varepsilon)$, as given in (18). Equivalently, one may revert to using the physical temperature:

$$T_1(\varepsilon) = \kappa\,\alpha_1(\varepsilon) + T_0 \qquad (20)$$

is the corresponding critical temperature of the upper transition. This critical temperature is isotropic and independent of Φ.

However, the fact that α_1 depends linearly in ε is itself an experimental signature for the nematic superconducting order. A single-component order parameter cannot couple linearly to $\vec{\varepsilon}$, as there is no way to form a combination that is invariant under threefold rotation.

The specific heat jump will be anisotropic. Following standard analysis, one recovers

$$\Delta c_{v,1} = \frac{\kappa^2}{2T_1(\varepsilon)} \frac{1}{\beta - \varepsilon\,[g_1 + g_2\cos(6\Phi)]}. \qquad (21)$$

This sixfold anisotropy is another unique signature of the nematic superconducting state. It shares similar physical origin with the predicted sixfold anisotropy of H_{c2} [22–24]: the external field sees only the underlying lattice as the source of anisotropy. By mapping out the ε and Φ dependence of $\Delta c_{v,1}$, one can in principle experimentally determine the Ginzberg-Landau coefficients involved. In particular, the the relative

size of $g1$ and $g2$ can be used to predict whether a lower transition may exist.

B. Middle transition

The existence of a middle transition is another unique signature of the nematic superconducting state. It separates the $\theta = 0$ phase from $\theta \neq 0$. Therefore θ itself is an appropriate order parameter to describe this transition. To this end, it is useful to first minimize $\mathcal{F}$ with respect to variation in D. Thus we define $\tilde{D}$ such that

$$\left(\frac{\partial \mathcal{F}}{\partial D}\right)_{D=\tilde{D}} = 0. \quad (22)$$

$\tilde{D}$ is an implicit function of θ, α, ε, and Φ. We will assume that the stress orientation is tuned to $\Phi = 0$ for the remainder of this part.

One can now derive a Ginzberg-Landau expansion for θ by replacing D with $\tilde{D}$:

$$\tilde{\mathcal{F}} \equiv a\tilde{D} + b\tilde{D}^2 + c\tilde{D}^3 = k_0 + k_2\,\theta^2 + k_4\,\theta^4 + \cdots. \quad (23)$$

Then the standard analysis of second order phase transition applies.

As noted in the previous section, the middle transition is due to the competition between g_0 and γ_2. It can be shown that, for asymptotically small ε, the leading expressions of coefficients k_2 and k_4 are independent of g_1 and g_2. Here we present these asymptotic formulas, though the exact analytic result can be obtained by carefully retaining all terms.

The critical temperature T_2 is

$$T_2 = T_0\left[1 - \frac{2}{3}\frac{\beta}{\kappa}\sqrt{\frac{g_0}{\gamma_2}}\sqrt{\varepsilon} + \frac{g_0}{\kappa}\left(\frac{2\gamma_2 - \gamma_1}{3\gamma_2}\right)\varepsilon\right], \quad (24)$$

and the specific heat jump is

$$\Delta c_{v,2} = \frac{\kappa^2 T_2(\varepsilon)}{T_0^2} \frac{9\,\gamma_2\,g_0\,\varepsilon}{8\beta^2\sqrt{\gamma_2 g_0 \varepsilon} + 2\beta(8\gamma_1 - \gamma_2)g_0\varepsilon + \frac{2}{\sqrt{\gamma_2}}[5 + (\gamma_1/\gamma_2) - 4(\gamma_1/\gamma_2)^2](g_o\varepsilon)^{5/2}}. \quad (25)$$

The formulas (24) and (25) are accurate in the limit where $(g_1\,\varepsilon/\beta)$, $(g_2\,\varepsilon/\beta)$, $g_1\sqrt{\varepsilon/g_0\,\gamma_2}$, and $g_2\sqrt{\varepsilon/g_0\,\gamma_2}$ are small.

It is worth pointing out that, around T_0 where the upper and middle transition merge, Eq. (24) implies

$$(T_2 - T_0) \propto \sqrt{\varepsilon}. \quad (26)$$

In particular, the T_2 line has an infinite slope at $\epsilon \to 0$. Generally it is thermodynamically forbidden for two lines of second order transition with *finite* slopes to meet and form a kink [50]. However, observing that the specific heat jump at the upper transition is the same for $\epsilon \to 0_\pm$, one can invoke thermodynamic arguments similar to that in [50] to show that T_2 must possess an infinite slope, and then this is an exception to the aforementioned "no-go" theorem.

We also note that $\Delta c_{v,2}$ vanishes in the limit $\varepsilon \to 0$. This is consistent with the sum rule

$$\lim_{\varepsilon \to 0}(\Delta c_{v,1} + \Delta c_{v,2}) = \Delta c_v, \quad (27)$$

where Δc_v is the specific heat jump of the superconducting transition at zero stress.

V. LOWER TRANSITION

The existence of a lower transition can be inferred by looking at the extremely low temperature $\alpha \to -\infty$ limit:

$$\begin{aligned}\tilde{\mathcal{F}} \approx &|\alpha|^{3/2}[3\gamma_1 + 3\gamma_2\cos(6\theta)] \\ &+ \frac{|\alpha|\{\beta - \varepsilon[g_1\cos(2\theta - 2\Phi) + g_2\cos(4\theta + 2\Phi)]\}}{3} \\ &\times [\gamma_1 + \gamma_2\cos(6\theta)] + O(|\alpha|^{1/2}).\end{aligned} \quad (28)$$

The leading term has the sixfold rotational symmetry, favoring all natural minima equally. The subleading term lifts this degeneracy.

The sign of $(g_1 - g_2)$ controls the qualitative behavior of (28). First assuming a generic value of Φ that breaks the sixfold rotational symmetry. If $g_1 > g_2$, out of the three minima, the one *closest* to Φ wins out. Conversely if $g_1 < g_2$, the minimum *furthest away* from Φ becomes the lowest. On the other hand, the order parameter has $\theta = \Phi$ at the upper transition, and then initially drifts toward the nearest of the natural minima as the temperature is lowered. For $g_1 < g_2$, there must be a first order transition separating the low-temperature asymptotic behavior from that just below the upper transition. This justifies (19) as the criterion for a lower transition.

The cases of $\Phi = 0$ and $\pi/6$ require special attention. For the sake of clarity, we introduce $\sigma = (\theta - \Phi)$, and consider the range $-\pi/2 < \sigma \leqslant \pi/2$. It can be shown that $\tilde{\mathcal{F}}$ exhibits the following properties at $\Phi = 0$ or $\pi/6$:

(1) $\tilde{\mathcal{F}}$ is symmetric under $\sigma \to -\sigma$.

(2) $\tilde{\mathcal{F}}$ is always stationary at $\sigma = \pi/2$ and 0.

(3) $\tilde{\mathcal{F}}$ admits at most five stationary points within the range $-\pi/2 < \sigma < \pi/2$ [51].

(4) Just below the upper transition, $\sigma = 0$ is the global minimum of $\tilde{\mathcal{F}}$, and $\sigma = \pi/2$ is the global maximum.

First let us look at the $\Phi = 0$ case. Coming down from high temperature, σ is initially fixed at 0, but drifts away from this high-symmetry direction below the middle transition. The previous argument for generic value of Φ therefore applies equally. However, below the lower transition, the location of global minimum in this case is pinned *exactly* at $\sigma = \pi/2$ by the enhanced symmetry.

Now we turn to the case of $\Phi = \pi/6$. As noted in the previous section, the lower transition here may be either first or second order.

If the lower transition is first order, $\tilde{\mathcal{F}}$ must develop a maximum-minimum pair on each side of $\sigma = 0$ as the temperature is lowered. This already accounts for five stationary points within $-\pi/2 < \sigma < \pi/2$, and $\sigma = 0$ must always remain a local minimum. On the other hand, a second order lower transition implies the stationary point at $\sigma = 0$ must

revert its character as the temperature is lowered. Therefore the criterion separating first and second order transition is whether $(\partial^2 \tilde{\mathcal{F}}/\partial \sigma^2)_{\sigma=0}$ changes sign when the temperature is lowered. This gives the critical stress:

$$\varepsilon_c = \frac{36 \, g_0 \gamma_3}{(g_1 - 4g_2)^2}. \tag{29}$$

If $\varepsilon > \varepsilon_c$, the lower transition becomes second order.

Finally, we will address the question of if and when the middle transition at $\Phi = 0$ ends on the surface of the lower transition. While a closed-form analytic solution is possible, the full expression is extremely long and unwieldy. We instead supply a recipe here.

The line of middle transition $\alpha_2(\varepsilon)$ is implicitly defined by

$$\left(\frac{\partial^2}{\partial \sigma^2} \tilde{\mathcal{F}}(\alpha = \alpha_2, \varepsilon, \sigma, \Phi = 0) \right)_{\sigma=0} = 0. \tag{30}$$

Since the phase below the lower transition has exactly $\sigma = \pi/2$ at $\Phi = 0$, the equation

$$\tilde{\mathcal{F}}(\alpha_2(\varepsilon_*), \varepsilon_*, \sigma = 0, \Phi = 0)$$
$$= \tilde{\mathcal{F}}(\alpha_2(\varepsilon_*), \varepsilon_*, \sigma = \pi/2, \Phi = 0) \tag{31}$$

determines the stress ε_* at which the middle and lower transitions meet if a solution exists. If there is no solution, then the line of the middle transition extends indefinitely into large ε. Our numerical results indicate that, depending on the actual values of GL coefficients, ε_* can be well within the limit (16), and the ending of the middle transition can be physically relevant.

VI. PREEXISTING PINNING FIELD AND SIGNATURES OF NEMATIC SUPERCONDUCTIVITY

As noted in the Introduction, there must be a preexisting SBF in the $M_x\mathrm{Bi_2Se_3}$ crystal to explain the pinning of the twofold anisotropic direction. Thus far we have assumed that mechanical stress is the only SBF present in our GL analysis. Should this be the case, one has direct control of the SBF by application of another external stress, and the predictions in the previous sections can be directly tested.

However, the true nature of the preexisting SBF is yet unknown, and it may not be mechanical stress or strain after all. In this section we consider the crystal subjected to both a *preexisting* pinning field $\vec{p}$ that is beyond our experimental control, and an *artificially applied* stress $\vec{\varepsilon}$ as an experimental probe.

The pinning field $\vec{p}$ must also transform under the E_g representation. In the same notation developed for stress, $\vec{p}$ can be expressed as

$$\vec{p} = p \begin{pmatrix} \cos(-2\Phi_p) \\ \sin(-2\Phi_p) \end{pmatrix} \equiv \begin{pmatrix} p_1 \\ p_2 \end{pmatrix}, \tag{32}$$

where the magnitude p is positive. In the absence of stress or any other external SBFs, the orientation of $\vec{\eta}$ is pinned at $\theta = \Phi_p$ near the superconducting T_c.

As discussed in the Introduction, the pinning effect is robust up to room temperature. Therefore we find it reasonable to model the $\vec{p}$ as essentially a given background, independent of temperature, near the superconducting T_c (≈ 3 K). While

$\vec{p}$ may itself depends on the applied stress, one can formally expand

$$\vec{p}(\vec{\varepsilon}) = \vec{p}(\vec{\varepsilon} = 0) + \cdots \tag{33}$$

and the higher order terms merely renormalizes the GL coefficients.

To our knowledge, the reported twofold anisotropy always aligns with a lattice direction in all known cases [14,17–19]. We therefore conjecture that the pinning field, whatever it may be, breaks the lattice symmetry by favoring one of the three twofold axes in the $\mathrm{Bi_2Se_3}$ structure.

The twofold axis of H_{c2} in transverse field at zero applied stress can be identified experimentally. We can redefine this twofold direction as the x axis. Following the analysis of [24], one deduces that the order parameter $\vec{\eta}$ is pinned at either the $(1,0)$ or $(0,1)$ direction. The (unknown) sign of the GL coefficient to a certain gradient term determines the correct choice. The two cases respectively yield

$$\vec{\eta} \propto (1,0), \quad \theta = \Phi_p = 0, \quad \vec{p} \propto (1,0); \quad \text{or}$$
$$\vec{\eta} \propto (0,1), \quad \theta = \Phi_p = \frac{\pi}{2}, \quad \vec{p} \propto (-1,0). \tag{34}$$

Now we consider how the system behaves when both the preexisting SBF $\vec{p}$ and the applied stress $\vec{\varepsilon}$ are present. We will focus on the split superconducting transition here, i.e., the pair of upper and middle transitions. To this end, one only needs to retain the coupling terms at order $O(\eta^2)$. The modified GL coupling terms reads

$$\mathcal{F}_p = -(g_0\vec{\varepsilon} + g_p\vec{p}) \cdot \vec{S}, \tag{35}$$

where S is given by (6).

We will define the so-called "total SBF" in the bulk of the superconductor as

$$\vec{P}_b \equiv g_0\vec{\varepsilon} + g_p\vec{p}, \tag{36}$$

with Φ_b the corresponding orientation angle. The GL free energy under consideration is

$$\mathcal{F} = [\alpha - |P_b| \cos(2\theta - 2\Phi_b)]D + \beta D^2 + \cdots. \tag{37}$$

The ratio g_p/g_0 is unknown. However, one can always make $\vec{\varepsilon} \propto (1,0)$ so that it is parallel to $\vec{p}$. Physically, this amounts to keeping $\varepsilon_2 = -2\varepsilon_{xy} = 0$ while varying $\varepsilon_1 = \varepsilon_{xx} - \varepsilon_{yy}$. The the change in magnitude $\Delta|P_b|$ is linearly dependent on the applied ε_1.

A. Upper transition

Following (18) and (20), the critical temperature of the upper (normal-to-superconducting) transition will show a kink when one continuously varies the applied stress:

$$(T_1 - T_0) \propto |P_b|. \tag{38}$$

This behavior is a unique signature of a nematic superconducting state. If the order parameter is single component, it cannot couple linearly to either stress or the SBF. One would expect instead a quadratic dependence:

$$(T_1 - T_0) \propto |P_b|^2. \tag{39}$$

In either case, the minimum of T_1 also marks the point where the twofold direction is tilted by $\pi/2$.

If the kink in (38) can be identified, the predicted sixfold anisotropy purely due to the lattice should be restored at that point. This effect can be seen from the specific heat jump, following (21). Following [24], the upper critical field H_{c2} should also exhibit the same sixfold anisotropy. This provides further verification for the nematic state.

B. Middle transition

The existence of the middle transition is another unique signature of the nematic superconducting state. Recall that it is due to the competition between the naturally preferred alignment of $\vec{\eta}$ and the explicit SBF.

We have been assuming that η_y is the naturally preferred order parameter, or that the GL coefficient γ_2 is positive. The middle transition exists when the orientation of the total SBF obeys $\Phi_b = 0$, or $\vec{P}_b \propto (1, 0)$, which is satisfied on only one side of the $|P_b| = 0$ kink. The second order phase transition may in principle be identified by the jump in specific heat (25).

We have made two assumptions here: the natural preferred direction, and the orientation of the preexisting pinning field (34). First, it may well be that η_x is the natural preference instead, but the conclusion that the middle transition exists on only one side of the $|P_b| = 0$ kink stands unaltered.

It is trickier if the preexisting $\vec{p}$ does not in fact align with a lattice direction. Should this turns out to be the case, one can instead apply both nonzero ε_1 and ε_2, keeping the ratio $\varepsilon_1/\varepsilon_2$ constant. The $\Phi_b = 0$ condition is satisfied by exactly one value of the magnitude ε, and the middle transition exists only at that point. Nevertheless, just off that exact value, the sharp middle transition is smeared into a crossover, and one can still register a steep increase in specific heat as an experimental signature.

VII. JOSEPHSON JUNCTION WITH AN *s*-WAVE SUPERCONDUCTOR

In this section we change gear slightly and discuss the phenomenology of tunneling current between a nematic superconductor and an *s*-wave superconductor. As pointed out by Yip *et al.* [43], one may write down the effective Hamiltonian of a junction purely based on symmetry considerations, in the same spirit of the GL theory. The behavior of the critical current then reflects the symmetry of the nematic order parameter. Here the implicit assumption is that the interface itself has spin-orbit coupling [52] so as to allow a tunneling supercurrent.

The theory for Josephson tunneling between two *s*-wave superconductors was worked out in the classic paper by Ambegaoker and Baratoff (AB) [53]. For a junction between two different *s*-wave superconductors, right below the lower of the two critical temperatures, the critical current is proportional to $\sqrt{T_c - T}$, and shows no strong stress dependence. In this section we explore how the proposed nematic superconducting state gives rise to qualitative differences.

We consider the scenario where an *s*-wave superconductor (with a much higher T_c) is attached to the $M_x\text{Bi}_2\text{Se}_3$ sample being tested. The surface contact of the sample is cut perpendicular to the z axis. We assume that the junction is in the tunneling limit.

The twofold rotation C_2' (and space inversion) in the original D_{3d} group is no longer a valid symmetry on the surface of contact. We will denote the reduced symmetry group as G. The junction coupling term in the effective Hamiltonian respects G, and of course the $U(1)$ gauge symmetry.

The *s*-wave superconductor is described by a complex scalar order parameter $\Psi = e^{i\chi}|\Psi|$. We make the gauge choice so that the order parameter $\vec{\eta}$ is real, and χ represents the phase difference between the two superconductors.

A. The intrinsic contribution

Let us first discuss the leading order junction term that is independent of any SBF. One can form G-invariant combinations at order $O(\eta^3)$, but these are not gauge invariant in their own right, and must be coupled to Ψ. And then the time-reversal symmetry demands the coupling terms to be overall Hermitian. The leading coupling term, at $O(\Psi)$ and $O(\eta^3)$, has the form

$$\begin{aligned} \mathcal{F}_{j0} &= m_0 \Psi^* (\eta_x S_2 - \eta_y S_1) + \text{H.c.} \\ &= m_0 \Psi^* (\vec{\eta} \wedge \vec{S}) + \text{H.c.}, \end{aligned} \tag{40}$$

where S is defined in (6). The coefficient m_0 must be real to satisfy time-reversal symmetry.

Here we assume that the junction is but a small perturbation to the bulk, and that the system is sufficiently close to the upper transition. One may therefore use the unperturbed solution for the nematic order parameter $\vec{\eta}$. Then the coupling (40) reduces to

$$\mathcal{F}_{j0} = -m_0 |\Psi| D^{3/2} \sin(3\theta) \cos(\chi), \tag{41}$$

where θ is the orientation of the order parameter $\vec{\eta}$ in the bulk.

The supercurrent across the junction can be identified [43] as $2(\partial \mathcal{F}_{j0}/\partial \chi)$. The factor of 2 is due to that the order parameters in the GL theory describe Cooper pairs. Using also the fact that $D \propto |\alpha|$ just below the upper transition, one can identify the critical current across the junction:

$$I_{c0} \propto (T_1 - T)^{3/2} |\sin 3\theta|. \tag{42}$$

In the hypothetical case where no SBF is present, (42) is the only contribution to the critical current. Our default scenario is that η_y is naturally preferred, or that $\theta = \pi/2$ here. Then (42) shows a 3/2 power-law temperature dependence that is markedly different from the AB theory. The other scenario is that $\theta = 0$, and tunneling is completely disallowed, again a drastic departure from the AB theory. When the total SBF in the bulk $\vec{P}_b$ is nonvanishing, $\theta = \Phi_b$ in the immediate vicinity of the upper transition.

B. The SBF-assisted contribution

The quantity S can be replaced by any SBF to yield an invariant coupling term. Here we will impose both a preexisting $\vec{p}$ and an applied stress $\vec{\varepsilon}$. The coupling term is thus

$$\mathcal{F}_{j1} = \Psi^* \vec{\eta} \wedge (m_p \vec{p} + m_\varepsilon \vec{\varepsilon}) + \text{H.c.} \tag{43}$$

Again, m_p and m_ε are real by time-reversal invariance.

Unfortunately, the ratio m_p/m_ε is not necessarily the same as g_0/g_ε. One defines another "total" SBF for the junction:

$$\vec{P}_j \equiv m_p \vec{p} + m_\varepsilon \vec{\varepsilon}, \tag{44}$$

which is in general not aligned with $\vec{P}_b$ in the bulk.

Let Φ_j be the orientation angle corresponding to $\vec{P}_j$. Again using the bulk solution for $\vec{\eta}$, (43) becomes

$$\mathcal{F}_{j1} = -\Psi^*|P_j|/\sqrt{D} \, \sin(\theta + 2\Phi_j)\cos\chi. \tag{45}$$

For a nonzero $|P_j|$, (45) is dominant in the immediate vicinity of the upper transition, where D is still small. Taking this limit, the critical current is

$$I_{c1} \propto |P_j|(T_1 - T)^{1/2}|\sin(\theta + 2\Phi_j)|. \tag{46}$$

If $\vec{\varepsilon}$ and $\vec{p}$ are not aligned, the angles Φ_b and Φ_j are different in general. This critical current therefore shows a twofold anisotropy as one rotates the stress, and has the conventional square-root dependence on temperature. At first sight, this tunneling current may seem indistinguishable from that of the anisotropic s-wave scenario, but there are still some dramatic signatures that are direct consequences of the nematic superconductivity.

C. Experimental signatures

At zero applied stress and nonvanishing preexisting pinning field, one has $\theta = \Phi_b = \Phi_j = \Phi_p$. We proceed to discuss the two cases in our conjecture (34) separately.

If $\Phi_p = 0$, then at zero applied stress, both I_{c0} and I_{c1} vanish, and there is no tunneling current allowed. An applied stress at a generic direction tilts both $\theta = \Phi_b$ and Φ_j, and turns on the tunneling current.

Alternatively, one keeps $\varepsilon_2 = 0$ and applies a nonzero ε_1 as proposed in the previous section. Φ_b and Φ_j go from 0 to $\pi/2$ as $\vec{P}_b$ and $\vec{P}_j$ crosses zero, respectively. While this change in Φ_j does not affect the critical currents, the change in Φ_p switches on the tunneling current from zero.

On the other hand, if $\Phi_p = \pi/2$, tunneling current without applied stress is initially nonzero. One again applies ε_1 while keeping $\varepsilon_2 = 0$. When $\vec{P}_b$ crosses zero, the tunneling current is switched off.

Additionally, if one finds a region where $\vec{P}_j \approx 0$ while $\Phi_b = \pi/2$, then $\mathcal{F}_{j1}$ is anomalously suppressed by the fine tuning of the applied stress, and the critical current will instead show the 3/2 power-law temperature dependence of I_{c0}.

The above treatment amounts to the direct coupling of the two superconducting bulks. This is admittedly an oversimplification: for unconventional superconductors, surface depairing may occur depending on the exact detail of the gap function [54]. The extent of this surface effect is dictated by the coherence length. Therefore, near T_c when the coherence length is large, surface depairing may substantially suppress the tunneling current; the overall temperature dependence will then have a higher power [38,55] than our simple prediction of 3/2. Nonetheless, the temperature dependence is clearly distinct from the s-wave-to-s-wave case.

D. $\vec{\eta}$ in E_g representation

As advertised in the Introduction, if $\vec{\eta}$ is instead even under space inversion, i.e., in the E_g representation, the results in this section need minor modifications. This stems from the fact that M, the mirror reflection about the yz-plane, acts differently on E_u and E_g. The coupling terms $\mathcal{F}_{j0}$ and $\mathcal{F}_{j1}$ becomes

$$\mathcal{F}_{j0}{}' = m_0 \Psi^*(\vec{\eta} \cdot \vec{S}) + \text{H.c.},$$
$$\mathcal{F}_{j1}{}' = \Psi^* \vec{\eta} \cdot (m_p \vec{p} + m_\varepsilon \vec{\varepsilon}) + \text{H.c.} \tag{47}$$

The upshot is that sines are to be replaced by cosines in both I_{c0} and I_{c1}:

$$I_{c0}{}' \propto (T_1 - T)^{3/2}|\cos 3\theta|,$$
$$I_{c1}{}' \propto |P_j|(T_1 - T)^{1/2}|\cos(\theta + 2\Phi_j)|. \tag{48}$$

The experimental signatures proposed above are still available, but all angles involved are shifted by $\pi/2$. Without an applied stress $\vec{\varepsilon}$, now tunneling current is forbidden at $\Phi_p = \pi/2$, and a nonzero $\vec{\varepsilon}$ that tilts $\vec{P}_j$ away switch on the current. On the other hand, $\Phi_p = 0$ initially allows a tunneling current that can be switched off by reversing $\vec{P}_j$. The temperature dependence of I_{c0} can be observed by having $\Phi_b = 0$ and $|P_j| \approx 0$.

VIII. CONCLUSION

In this paper we explore the coupling between the two-component superconducting order parameter $\vec{\eta}$ and the (traceless part of) stress $\vec{\varepsilon}$ in the basal plane, and map out possible phase diagrams allowed by symmetry constraints. Indeed the analysis is not restricted to mechanical stress: any SBF must couple in a similar manner. In later sections we consider the the case where there are a preexisiting pinning SBF in the sample, and an applied stress as an experimental probe.

In the presence of a SBF, we found that the superconducting transition splits into two (*upper* and *middle* transitions), and there may be another phase transition at an even lower temperature (*lower* transition), depending on the values of GL coefficients.

The critical temperature (20) of the upper transition does not show any anisotropy, but a *sixfold* anisotropy for the specific heat jump (21) is predicted as the SBF is rotated. The physics behind is similar to the theoretical angular dependence of upper critical field discussed in the literature [22–24].

The middle transition only exist when the SBF is aligned along $\Phi = 0$; the sharp transition becomes a crossover if the alignment is not exact. We give formulas for the transition temperature (24) and specific heat jumps (25). As the middle transition is connected to the superconducting transition without a symmetry breaking field, we expect that these results from our GL theory are still quantitatively accurate.

The same cannot be said for the lower transition, which is not connected to the superconducting transition without a SBF. The assumption that GL coefficients are temperature independent may no longer be a quantitatively accurate approximation, and we focus our effort on the qualitative results. The existence of a lower transition hinges on the criterion (19). It is first order almost everywhere, except when

$\Phi = \pi/6$ and $\varepsilon > \varepsilon_c$ it becomes second order. The critical value ε_c is given in (29).

The observed twofold anisotropy of H_{c2}, and the robust pinning of the twofold direction over many cycles, suggest that a preexisting pinning field explicitly breaks the rotational symmetry in the sample. We discuss how, at leading order in GL theory, the pinning field and an externally applied stress combine to form a "total" SBF felt by the sample. By varying the applied stress, one gains access to different regions of the three-dimensional phase diagram worked out above.

We point out two thermodynamics experimental signatures unique to the nematic state. First, the superconducting critical temperature is *linearly* proportional to the strength of the total SBF, as given in (38), as opposed to the quadratic relation if the order parameter is single component. Second, the existence of the middle transition, and the associated finite crossover even if the total SBF is not exactly tuned to the right orientation, can be observed through calorimetry experiments.

When linked to another *s*-wave superconductor, the Josephson tunneling current also offers hints to the superconducting pairing symmetry. We discuss how an applied stress can switch the tunneling current on and off if the superconducting order parameter is indeed nematic. The unusual $(T_1 - T)^{3/2}$ temperature dependence of critical current I_{c0} (42) may also be seen in experiment if the required conditions are met. None of these peculiar behaviors can be seen if the superconductivity of $M_x\text{Bi}_2\text{Se}_3$ turns out to be *s* wave.

We hope our findings here will guide future experimental effort in discerning the pairing symmetry of the Bi_2Se_3 family of superconductor, thereby helping to settle the debate on the topological nature of the superconductivity.

ACKNOWLEDGMENTS

[1] Y. Xia, D. Qian, D. Hsieh, L. Wray, A. Pal, H. Lin, A. Bansil, D. Grauer, Y. S. Hor, R. J. Cava, and M. Z. Hasan, Nat. Phys. **5**, 398 (2009).

[2] H. Zhang, C.-X. Liu, X.-L. Qi, X. Dai, Z. Fang, and S.-C. Zhang, Nat. Phys. **5**, 438 (2009).

[3] C.-X. Liu, X.-L. Qi, H. J. Zhang, X. Dai, Z. Fang, and S.-C. Zhang, Phys. Rev. B **82**, 045122 (2010).

[4] Y. S. Hor, A. J. Williams, J. G. Checkelsky, P. Roushan, J. Seo, Q. Xu, H. W. Zandbergen, A. Yazdani, N. P. Ong, and R. J. Cava, Phys. Rev. Lett. **104**, 057001 (2010).

[5] M. Kriener, K. Segawa, Z. Ren, S. Sasaki, and Y. Ando, Phys. Rev. Lett. **106**, 127004 (2011).

[6] Shruti, V. K. Maurya, P. Neha, P. Srivastava, and S. Patnaik, Phys. Rev. B **92**, 020506(R) (2015).

[7] Y. Qiu, K. N. Sanders, J. Dai, J. E. Medvedeva, W. Wu, P. Ghaemi, T. Vojta, and Y. S. Hor, arXiv:1512.03519.

[8] T. Asaba, B. J. Lawson, C. Tinsman, L. Chen, P. Corbae, G. Li, Y. Qiu, Y. S. Hor, L. Fu, and L. Li, Phys. Rev. X **7**, 011009 (2017).

[9] L. Fu and E. Berg, Phys. Rev. Lett. **105**, 097001 (2010).

[10] L. Fu, Phys. Rev. B **90**, 100509(R) (2014).

[11] J. W. F. Venderbos, V. Kozii, and L. Fu, Phys. Rev. B **94**, 180504(R) (2016).

[12] S. Yonezawa, Condens. Matter **4**, 2 (2018).

[13] K. Matano, M. Kriener, K. Segawa, Y. Ando, and G.-q. Zheng, Nat. Phys. **12**, 852 (2016).

[14] S. Yonezawa, K. Tajiri, S. Nakata, Y. Nagai, Z. Wang, K. Segawa, Y. Ando, and Y. Maeno, Nat. Phys. **13**, 123 (2017).

[15] K. Willa, R. Willa, K. W. Song, G. D. Gu, J. A. Schneeloch, R. Zhong, A. E. Koshelev, W.-k. Kwok, and U. Welp, Phys. Rev. B **98**, 184509 (2018).

[16] Y. Sun, S. Kittaka, T. Sakakibara, K. Machida, J. Wang, J. Wen, X. Xing, Z. Shi, and T. Tamegai, Phys. Rev. Lett. **123**, 027002 (2019).

[17] Y. Pan, A. M. Nikitin, G. K. Araizi, Y. K. Huang, Y. Matsushita, T. Naka, and A. de Visser, Sci. Rep. **6**, 28632 (2016).

[18] G. Du, Y. Li, J. Schneeloch, R. D. Zhong, G. Gu, H. Yang, H. Lin, and H.-H. Wen, Sci. China: Phys., Mech. Astron. **60**, 037411 (2017).

[19] M. P. Smylie, K. Willa, H. Claus, A. E. Koshelev, K. W. Song, W.-K. Kwok, Z. Islam, G. D. Gu, J. A. Schneeloch, R. D. Zhong, and U. Welp, Sci. Rep. **8**, 7666 (2018).

[20] T. V. Bay, T. Naka, Y. K. Huang, H. Luigjes, M. S. Golden, and A. de Visser, Phys. Rev. Lett. **108**, 057001 (2012).

[21] A. M. Nikitin, Y. Pan, Y. K. Huang, T. Naka, and A. de Visser, Phys. Rev. B **94**, 144516 (2016).

[22] D. F. Agterberg and M. B. Walker, Phys. Rev. Lett. **74**, 3904 (1995).

[23] P. L. Krotkov and V. P. Mineev, Phys. Rev. B **65**, 224506 (2002).

[24] J. W. F. Venderbos, V. Kozii, and L. Fu, Phys. Rev. B **94**, 094522 (2016).

[25] A. de Visser (private communication).

[26] M. P. Smylie (private communication).

[27] A. Y. Kuntsevich, M. A. Bryzgalov, V. A. Prudkoglyad, V. P. Martovitskii, Y. G. Selivanov, and E. G. Chizhevskii, New J. Phys. **20**, 103022 (2018).

[28] M. Hecker and J. Schmalian, npj Quantum Mater. **3**, 26 (2018).

[29] M. Sigrist and K. Ueda, Rev. Mod. Phys. **63**, 239 (1991).

[30] R. Joynt and L. Taillefer, Rev. Mod. Phys. **74**, 235 (2002).

[31] D. W. Hess, T. A. Tokuyasu, and J. A. Sauls, J. Phys.: Condens. Matter **1**, 8135 (1989).

[32] K. Machida and M.-a. Ozaki, J. Phys. Soc. Jpn. **58**, 2244 (1989).

[33] R. A. Fisher, S. Kim, B. F. Woodfield, N. E. Phillips, L. Taillefer, K. Hasselbach, J. Flouquet, A. L. Giorgi, and J. L. Smith, Phys. Rev. Lett. **62**, 1411 (1989).

[34] M. Sigrist, R. Joynt, and T. M. Rice, Phys. Rev. B **36**, 5186 (1987).

[35] M. B. Walker and P. Contreras, Phys. Rev. B **66**, 214508 (2002).

[36] C. W. Hicks, D. O. Brodsky, E. A. Yelland, A. S. Gibbs, J. A. N. Bruin, M. E. Barber, S. D. Edkins, K. Nishimura,

S. Yonezawa, Y. Maeno, and A. P. Mackenzie, Science **344**, 283 (2014).

[37] C. A. Watson, A. S. Gibbs, A. P. Mackenzie, C. W. Hicks, and K. A. Moler, Phys. Rev. B **98**, 094521 (2018).

[38] Y. Tanaka and S. Kashiwaya, Phys. Rev. B **56**, 892 (1997).

[39] A. Sumiyama, S. Shibata, Y. Oda, N. Kimura, E. Yamamoto, Y. Haga, and Y. Onuki, Phys. Rev. Lett. **81**, 5213 (1998).

[40] Y. Tanaka and S. Kashiwaya, Superlattices Microstruct. **25**, 1083 (1999).

[41] N. Stefanakis, Phys. Rev. B **65**, 064533 (2002).

[42] J. Gouchi, A. Sumiyama, G. Motoyama, A. Yamaguchi, N. Kimura, E. Yamamoto, Y. Haga, and Y. Ōnuki, J. Phys. Soc. Jpn. **81**, 113701 (2012).

[43] S.-K. Yip, O. F. De Alcantara Bonfim, and P. Kumar, Phys. Rev. B **41**, 11214 (1990).

[44] Y. Ando, K. Segawa, S. Komiya, and A. N. Lavrov, Phys. Rev. Lett. **88**, 137005 (2002).

[45] V. Hinkov, D. Haug, B. Fauque, P. Bourges, Y. Sidis, A. Ivanov, C. Bernhard, C. T. Lin, and B. Keimer, Science **319**, 597 (2008).

[46] R. Daou, J. Chang, D. LeBoeuf, O. Cyr-Choinière, F. Laliberté, N. Doiron-Leyraud, B. J. Ramshaw, R. Liang, D. A. Bonn,

W. N. Hardy, and L. Taillefer, Nature (London) **463**, 519 (2010).

[47] Y. Sato, S. Kasahara, H. Murayama, Y. Kasahara, E.-G. Moon, T. Nishizaki, T. Loew, J. Porras, B. Keimer, T. Shibauchi, and Y. Matsuda, Nat. Phys. **13**, 1074 (2017).

[48] G. E. Volovik, Pis'ma Zh. Eksp. Teor. Fiz. **48**, 39 (1988) [JETP Lett. **48**, 41 (1988)].

[49] D. F. Agterberg and M. B. Walker, Phys. Rev. B **51**, 8481 (1995).

[50] S. K. Yip, T. Li, and P. Kumar, Phys. Rev. B **43**, 2742 (1991).

[51] To see this, one notes that for a given σ, the relationship between $\tilde{D}$ and α is invertible. Instead of finding an upper bound on number of stationary points along the path of constant α and ε, one may solve for the much easier case of constant $\tilde{D}$ and ε.

[52] A. Millis, D. Rainer, and J. A. Sauls, Phys. Rev. B **38**, 4504 (1988).

[53] V. Ambegaokar and A. Baratoff, Phys. Rev. Lett. **10**, 486 (1963).

[54] S. Yip, Y. Sun, and J. Sauls, Czech. J. Phys. **46**, 557 (1996).

[55] S.-K. Yip, J. Low Temp. Phys. **109**, 547 (1997).